

Haptics Electromyography Perception and Learning Enhanced Intelligence for Teleoperated Robot

Chenguang Yang^{id}, *Senior Member, IEEE*, Jing Luo^{id}, *Student Member, IEEE*,
Chao Liu^{id}, *Senior Member, IEEE*, Miao Li, and Shi-Lu Dai^{id}, *Member, IEEE*

Abstract—Due to the lack of transparent and friendly human–robot interaction (HRI) interface, as well as various uncertainties, it is usually a challenge to remotely manipulate a robot to accomplish a complicated task. To improve the teleoperation performance, we propose a new perception mechanism by integrating a novel learning method to operate the robots in the distance. In order to enhance the perception of the teleoperation system, we utilize a surface electromyogram signal to extract the human operator’s muscle activation. As a response to the changes in the external environment, as sensed through haptic and visual feedback, a human operator naturally reacts with various muscle activations. By imitating the human behaviors in task execution, not only motion trajectory but also arm stiffness adjusted by muscle activation, it is expected that the robot would be able to carry out the repetitive tasks autonomously or uncertain tasks with improved intelligence. To this end, we develop a robot learning algorithm based on probability statistics under an integrated framework of the hidden semi-Markov model (HSMM) and the Gaussian mixture method. This method is employed to obtain a generative task model based on the robot’s trajectory. Then, Gaussian mixture regression based on HSMM is applied to correct the robot trajectory with the reproduced results from the learned task model. The execution procedures consist of a *learning phase* and a *reproduction phase*. To guarantee the stability, immersion, and maneuverability of the teleoperation system, a variable gain control method that involves electromyography (EMG) is introduced. Experimental results have demonstrated the effectiveness of the proposed method.

Note to Practitioners—This paper is inspired by the limitations of teleoperation to perform a task with unfriendly HRI and

lack of intelligence. The human operators need to concentrate on the manipulation in the traditional setup of a teleoperation system; thus, it is quite a labor intensive for a human operator. This is a huge challenge for the requirement of increasingly complicated, diverse tasks in teleoperation. Therefore, efficient ways of the robot intelligence need to be urgently developed for the telerobots. In this paper, we develop a robot intelligence framework by merging robot learning technology and perception mechanism. The proposed framework is effective where the task performed with repeatability and rapidity in a teleoperated mode. The proposed method includes three following ideas: 1) remote operation information can be actively sensed by infusing muscle activation with a haptics EMG perception mechanism; 2) the robot intelligence can be enhanced by employing a robot learning method. The developed approach is verified by the experimental results; and 3) the proposed method can be potentially used for telemanufacturing, telehabilitation, and telemedicine, and so on. In our future work, more interactive information between humans and telerobots should be taken into consideration in the telerobot perception system to enhance the robot intelligence.

Index Terms—Gaussian mixture model (GMM), haptics electromyography (EMG) perception, hidden semi-Markov model (HSMM), human–robot interaction (HRI), robot intelligence, teleoperated robot learning.

I. INTRODUCTION

PROPELLED by sensor technologies, computer technologies, control technologies, and mechatronic design, the intelligent robots have made a breakthrough over the past three decades [1], [2]. Nowadays, the robots have been widely used in industry because of its high versatility and adaptability [3], [4]. With the expansion of its application in various areas, the collaborative working environments of robots are being more complicated, and the complexity level of tasks has also greatly increased [5], [6]. However, the development of robot technology has not been broadly consistent with human expectations. Related studies demonstrate that the autonomous robot system cannot accomplish a task in an unknown or a complicated environment in the foreseen future with the limitations of sensor, control, artificial intelligence, and mechanism. Therefore, the telerobot based on human–robot interaction (HRI) is a realistic option to manipulate a complex task by allocating the human intelligence and robot’s capabilities to enhance the robot intelligence [7]–[9]. As shown in Fig. 1, a possible human-in-the-loop teleoperation system consists of the following modules: human operator, information perception interface, task learning, and task reproduction. The human operator is the main factor for the telerobot [10], [11]. The information perception module

Manuscript received June 8, 2018; revised August 17, 2018; accepted September 21, 2018. Date of publication October 29, 2018; date of current version October 4, 2019. This paper was recommended for publication by Associate Editor H. Liu and Editor H. Liu upon evaluation of the reviewers’ comments. This work was supported in part by the National Nature Science Foundation under Grant 61473120, Grant 61811530281, Grant 61473121, and Grant 51705371, in part by the Science and Technology Planning Project of Guangzhou under Grant 201607010006 and Grant 201604016082, in part by the State Key Laboratory of Robotics and System under Grant SKLRS-2017-KF-13, in part by the Fundamental Research Funds for the Central Universities under Grant 2017ZD057, and in part by Guangdong Natural Science Foundation under Grant 2017A030313381. (*Corresponding author: Shi-Lu Dai.*)

C. Yang, J. Luo, and S.-L. Dai are with the Key Laboratory of Autonomous Systems and Networked Control, School of Automation Science and Engineering, South China University of Technology, Guangzhou 510640, China (e-mail: cyang@ieee.org; jingluo.ac@gmail.com; audaisl@scut.edu.cn).

C. Liu is with the Department of Robotics, LIRMM, UMR5506, University of Montpellier-CNRS, 34095 Montpellier, France (e-mail: liu@lirmm.fr).

M. Li is with the School of Power and Mechanical Engineering, Wuhan University, Wuhan 430074, China (e-mail: miao.li@whu.edu.cn).

Color versions of one or more of the figures in this article are available online at <http://ieeexplore.ieee.org>.

Digital Object Identifier 10.1109/TASE.2018.2874454

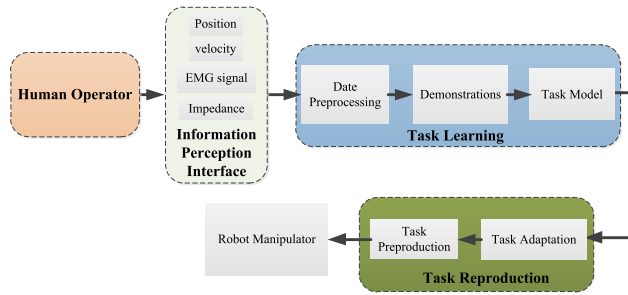


Fig. 1. Information perception and robot learning for the teleoperation system.

is used to provide a perception platform for information deliver between the human operator and the robot [12]. The operator's physical or physiological information [i.e., motion, electromyography (EMG), etc.] can be used to enhance the capability of HRI. When the human operator receives the feedback from the external environment, the human operator can actively adjust muscle activation via EMG signals to cope with the change in the external environment. The task learning module is mainly used to learn a specific skill through HRI. The robot reproduction module recognizes the current task initial situations and updates the generative task model to improve the manipulation performance.

Given the precise information, including work environments and mission scenarios, the telerobots can be programmed by the means of code by an expert or an experienced operator in industrial fields for tasks such as automatic spraying, automatic welding, and automatic guided vehicle. This programming method is widely applied in many areas that require high precision, high speed, and high repeatability. Alternatively, the robot learning is a method that the robot can learn to perform a certain task via HRI and to reduce the burden of the operator to meet the demand of efficiency in the industrial field. This learning method is also called programming by demonstration or learning from demonstration. Generally speaking, the robots learn a specific task through direct demonstration of human teleoperating a robot, 3-D vision teaching, virtual demonstration, and so on. The human operators teach the robots to exploit a specific skill by using the interaction information, such as interaction force, position, visual images, voice, physiological signals of the human, and so on. There are a number of algorithms dedicated to the study of the topic of robot learning. Robot learning methods can be divided into two groups: the perception system level and the learned task level. The perception system involves vision and perceptible motion, while the learned task level comprises the task trajectories or hidden state information (position, velocity, force, and human intention) [13], [14]. Vision perception system is an effective way to capture the information of HRI [15]–[19]. Chalodhorn *et al.* [15] proposed a learned sensory-motor model for a humanoid robot to learn human gait via motion capture system. Grollman and Jenkins [17] used a perception system to collect the data for the purpose of the robot imitation. In addition, many researchers employed

motion sensors to capture human motion to teach the robots to manipulate a specific task [18], [19].

In addition, by extracting the information from a demonstrated trajectory could also facilitate robot learning. Field *et al.* [20] presented a method by learning a joint space trajectory model for robot programming. In [21], a complex trajectory reproduction method is used to transfer the knowledge of a human to a robot by demonstration. A similar learning model was presented in [22]. Especially, Deniša *et al.* [23] developed a compliant movement primitives method to encode the position trajectory for robot learning. In order to improve the performance of robot programming, related researchers have proposed a number of methods at the robot learning phase. Racca *et al.* [24] proposed a method integrated hidden semi-Markov model (HSMM) with Cartesian impedance control to perform the complex tasks like opening a door or manipulating a button. In [25], a parametric hidden Markov model (HMM) was used to encode the data from the demonstrations in the training phase. Tanwani and Calinon [26], [27] developed a task-parameterized HSMM to copy with the environmental situations in the process of manipulation tasks. From the above-mentioned works, the robot learning can be regarded as a problem of feature extraction from the demonstrated training data for a specific skill in the process of HRI. By using robot learning, the robot can obtain a task model which embeds human intention. Khokar *et al.* [28] used HMMs to recognize human motion intention by an expert with offline training. Stefanov *et al.* [29] extracted features from the haptic device and adopted HMM algorithm to achieve human intention recognition through classification. In [30], an Intention-Driven Dynamics Model was presented to infer human intentions from observed motions. Maeda *et al.* [31] developed an interaction learning method to generate a collaborative trajectory from human movement observations. Ravichandar and Dani [32] proposed an adaptive-neural-intention estimator method to recognize the operator's motion intention by using the observations via offline training and online intention estimation. For teleoperated robots, a human operator is regarded as a factor to perform tasks cooperatively [28], [33], [34]. The human performance greatly decides the accomplishment of the task. Pervez *et al.* [35] presented a learning method based on dynamical movement primitives to manipulate the peg-in-hole task with a three DOF master-slave robot. However, influenced by an uncertain environment, it is difficult to utilize the human cognition for the manipulation of the task. In addition, the motion and command of the operator involve his/her perception and intention in the process of task collaboration [36].

In this paper, we combine the human intelligence with the robot's capability to ensure the performance of the task and to enhance the robot intelligence of the teleoperated robot. In the information perception interface, surface electromyogram (sEMG) signal is applied to detect the operator's muscle activation when the operator manipulates the haptic device to adapt to the external environments. For a specific skill, the muscle activation varies with the operator's movements/commands. In addition, representations of human-telerobot collaboration, such as trajectories of the

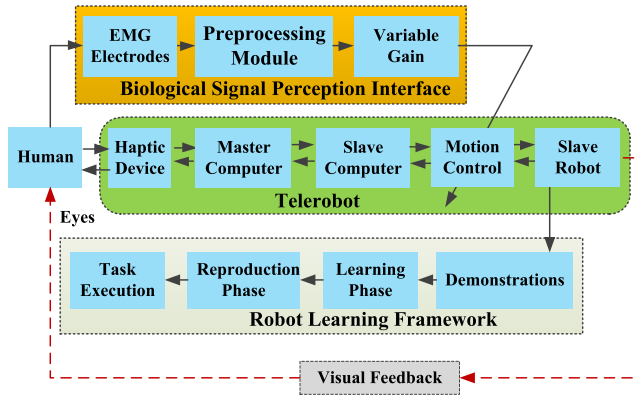


Fig. 2. Block diagram of a teleoperation system.

task/robot's end-effector, motion of the human, and variation of muscle activation, indicate a specific skill and human intention. First, by introducing a combined scheme of HSMM and Gaussian mixture model (HSMM-GMM), we can obtain a generative model in the *learning* phase. Similarly, in the *reproduction* phase, a task reproduction model is executed based on HSMM and Gaussian mixture regression (HSMM-GMR). Second, in the *learning* and *reproduction* phase, based on our previous work [37], a sEMG signal is embedded into control strategy to indicate the intentions of human control gain and movement. For the telerobot, it can learn how to actively use a suitable control gain to perform a task which is inspired by the human muscle activation according to the external environments. Finally, experimental studies are performed to show the effectiveness and superiority of the developed algorithms.

Section II presents preliminaries to introduce the teleoperated system and the sEMG signal processing. Section III presents the proposed task generative model in *learning* and *reproduction* phase. Section VI describes system dynamics and control strategy. The experimental setup and results are presented in Section V. Finally, Section VI concludes the work in this paper.

II. PRELIMINARIES

A. Teleoperation System Description

As shown in Fig. 2, a novel teleoperation system is developed in this paper. It includes three main modules: a biological signal perception interface module, a telerobot module, and a robot learning module.

- 1) *Biological Signal Perception Interface Module*: The biological signal perception interface module consists of sEMG electrodes, preprocessing unit, and a variable gain unit. This module is used to sense the human operator's muscle activation. The sampled sEMG information indicates the electrical activity of the hand muscle in the process of HRI. Through the signal processing module, an envelop line of the sEMG signal can be obtained. In this module, the obtained variable gain is used to control the motion of the slave.

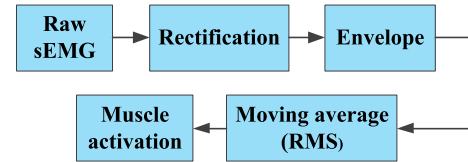


Fig. 3. Muscle activation descriptor based on sEMG signal.

- 2) *Telerobot Module*: The telerobot module is the main part of the frame which employs a master-slave structure. It can be observed in Fig. 2 that the slave device follows the master's motion generated by the human operator.
- 3) *Robot Learning Framework Module*: The robot learning module is responsible for both task learning and reproduction. In the learning phase, the telerobot obtains *a priori* knowledge task model to learn a specific skill from the human operator by using statistical learning theory. In the reproduction phase, the task model is updated according to the current situations, and the robot executes the updated task.

B. Muscle Activation Descriptor

Generally, the EMG signal is a result of the comprehensive effect of motor unit action potential of muscle fiber both in time and in space for surface muscle [38], [39]. The sEMG signals can be used in three applications: indicator of the muscle activation, representation of the force based on human muscle, and a descriptor of the fatigue for the muscle [38]. In this paper, we use the sEMG signal as the muscle activation descriptor. The process of sEMG signals preprocessing can be seen in Fig. 3.

In this paper, an MYO armband (Thalmic Labs Inc.) with $N = 8$ detection channels is used to sample the EMG signal by employing bluetooth communication technique

$$u = \sum_i^N u_{\text{raw}}(i), \quad N = 1, 2, 3, \dots, 8 \quad (1)$$

where $u_{\text{raw}}(i)$ and u are the raw sEMG signals and the sEMG signal, respectively.

Generally, the sEMG signal (blue) u involves noise. In order to extract the muscle activation from the sEMG as filtered as possible, the root mean square (rms) of the sEMG signal is applied in this paper as follows:

$$\text{rms} = \sqrt{\frac{1}{L_{\text{win}}} \sum_{i=1}^{L_{\text{win}}} u_i^2} \quad i = 1, 2, \dots, L_{\text{win}} \quad (2)$$

where L_{win} is the size of sampling moving window, rms presents the rms of the sEMG signal or the muscle activation of descriptor. The value of the rms represents the instantaneous electric power of the sEMG signal and reflects the effective value of the muscle surface electrodischarge. The size of the moving window is a parameter to tune according to experience for many times.

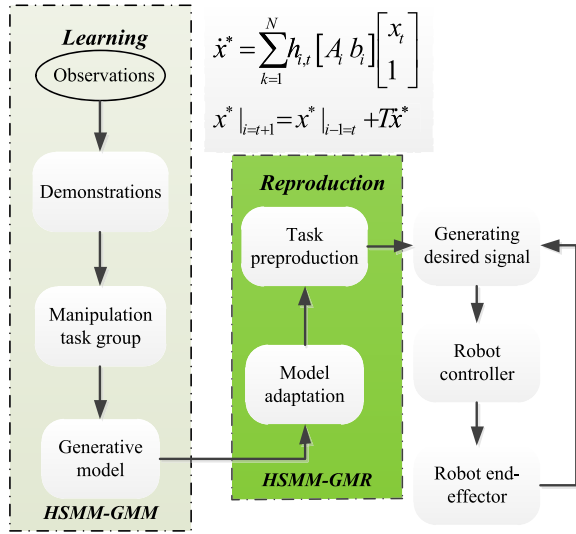


Fig. 4. Proposed task generative model.

III. ROBOT LEARNING MODEL

In the teleoperated systems, the performance of teleoperation is highly correlated with the human operator's skill. When the human operator performs a task through the teleoperated robot, the completion of task may be affected by the relationship with the external environment, the telerobot, and the human subjective initiative. In order to enhance the capability of HRI, a novel method is utilized to obtain a task model for the teleoperation.

In this paper, we select the end-effector of a slave device to perform a specific task trained with different initial conditions, e.g., different initial locations. We then obtain a task learning model by using the HSMM method.

The proposed task generative frame¹ is shown in Fig. 4. In the *learning* phase, based on the collected data of task from demonstrations, HSMM-GMM is used to obtain the task model parameters. In the *reproduction* phase, the telerobot behavior is reproduced based on HSMM-GMR according to a given task parameter set.

A. Parameters of Task Generative Model

The input data is collected by the positions x and velocities \dot{x} of the robot end-effector.²

Because the performance of task is demonstrated by the robot manipulator through the human operator, we define the pose of the slave device $\xi \in \mathbb{R}^D$ as an observation sequence with

$$\begin{cases} \xi = \begin{bmatrix} \xi^I \\ \xi^O \end{bmatrix} \\ x = x_s \end{cases} \quad (3)$$

¹As seen in Fig. 4, in the *reproduction* phase, T is equal to \mathcal{T} in the equations.

²To guarantee the accuracy of these data for task learning, we use the pose of end-effector of the slave device as input signals rather than the one of the master device.

where ξ^I is the pose of manipulator of the slave with the input components and ξ^O are out components, respectively. $x_s \in \mathbb{R}^3$ represents the position of the slave.

The task generative model incorporates six elements that are presented as follows:

1) *State of Model*: Suppose that there are N states or N hidden states in the HSMM, i.e., $S = [S_1, S_2, S_3, \dots, S_N]$. At time t , the hidden state is $q_t \in [S_1, S_2, S_3, \dots, S_N]$.

2) *Number of Observations*: M indicates the number of observation. A set V incorporates M observations is $V = [v_1, v_2, v_3, \dots, v_M]$. At time t , the observation is $o_t \in [v_1, v_2, v_3, \dots, v_M]$.

3) *Initial Probability Distribution Vector*: $\pi = [\pi_1, \pi_2, \pi_3, \dots, \pi_N]$ represents the initial probability distribution of model, it defines the probability distribution of each hidden state at the beginning of calculation $\pi_i = P(q_1 = S_i) \geq 0$, ($1 \leq i \leq N$) and satisfies $\sum_{i=1}^N \pi_i = 1$.

4) *Transition Probability Distribution Matrix*: $A = [a_{ij}]_{N \times N}$ is the transition probability distribution matrix for hidden state i at time $(t-1)$ to hidden state j at time t , i.e., $a_{ij} = P(q_{t+1} = S_j | q_t = S_i)$, ($1 \leq i, j \leq N$). It satisfies $\sum_{j=1}^N a_{ij} = 1$, ($1 \leq i \leq N$).

5) *Gaussian Mixture Parameters and Observation Probability Matrix*: We use the Gaussian joint probabilities to represent the output probability distribution for observation, i.e., $\mu = (\mu_1, \mu_2, \mu_3, \dots, \mu_i, \dots, \mu_N)$ and $\sigma = (\sigma_1, \sigma_2, \sigma_3, \dots, \sigma_i, \dots, \sigma_N)$, where $i \in [1, N]$. Therefore, the observation probability at time t for state S_i is $p_i(t) = \mathcal{N}(t; \mu_i, \sigma_i)$. $B = b_i(k)_{N \times M}$ indicates the observation probability matrix in state S_i , and $b_i(k) = P(o_t = v_k, q_t = S_i)$ ($1 \leq i \leq N, 1 \leq k \leq M$).

6) *Probability Density Function for State Dwell Time*: We train the model c times in a set $c \in \{1, 2, \dots, C\}$, and we have $\mu^C = (\mu_1^C, \mu_2^C, \mu_3^C, \dots, \mu_N^C)$ and $\sigma^C = (\sigma_1^C, \sigma_2^C, \sigma_3^C, \dots, \sigma_N^C)$, where μ^C and σ^C are the mean values and variances of the Gaussian duration probability distribution, respectively. The state duration probability density function $p_i^C(t)$ of state i is $p_i^C(t) = \mathcal{N}(t; \mu_i^C, \sigma_i^C)$.

Therefore, the proposed model with N states is parametrized by

$$\lambda = \{\pi, A, \{\mu, \sigma\}, \{\mu^C, \sigma^C\}\}_{i,j}^N. \quad (4)$$

B. Initialization of Task Generative Model

According to the above-mentioned specification, we need to initialize the model λ , i.e., the given values of parameters which are of reevaluation. Generally, the form of a Markov chain is determined by the parameters of model π and A . However, the initial values of both π and A have little impact on the final convergence effect of the model under the case of certainty for the Markov chain. In the parameters of the actual model, the initial value of the state duration probability density function $p_i^C(t)$ does affect the final results, but the influence is very limited. Therefore, the parameters of $\{\pi, A, p_i^C(t)\}$ can be initialized to be random or equal numbers. However, the parameters $\{\mu, \sigma\}$ have a big impact on the convergence property. We set the initial values of μ, σ with the K -means method [27], [40].

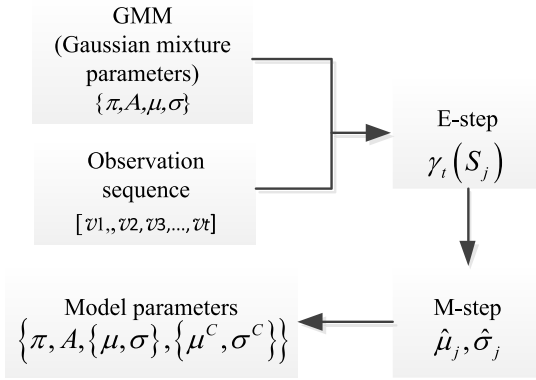


Fig. 5. Training of the model.

C. Training Method

The purpose of model training is to acquire the model parameters $\lambda = \{\pi, A, \{\mu, \sigma\}, \{\mu^C, \sigma^C\}\}$ according to a given observation sequence $V = [v_1, v_2, v_3, \dots, v_T]$ through the expectation-maximization algorithm [41]. We suppose that the observation obeys an independent Gaussian probability distribution in this paper. The process of training model is shown in Fig. 5.

According to the given observation sequence to evaluate the probability $\gamma_t(S_j)$ of state S_j at time t

$$\gamma_t(S_j) = P(S(t) = s_j | V, \lambda) = \frac{p(V, S(t) = s_j | \lambda)}{p(V | \lambda)}. \quad (5)$$

According to $\gamma_t(S_j)$ to reevaluate the parameters of model λ

$$\begin{cases} \hat{\mu}_j = \frac{\sum_{t=1}^T \gamma_t(S_j) v_t}{\sum_{t=1}^T \gamma_t(S_j)} \\ \hat{\sigma}_j = \frac{\sum_{t=1}^T \gamma_t(S_j) (v_t - \hat{\mu}_j)(v_t - \hat{\mu}_j)^T}{\sum_{t=1}^T \gamma_t(S_j)}. \end{cases} \quad (6)$$

D. Observation Constituent

We define the pose of the slave device ξ_t as an observation sequence with

$$\xi_t = \begin{bmatrix} \xi_t^I \\ \xi_t^O \end{bmatrix} \quad (7)$$

$$\mu_i = \begin{bmatrix} \mu_i^I \\ \mu_i^O \end{bmatrix} = \begin{bmatrix} \mu_i^x \\ \mu_i^y \end{bmatrix} \quad (8)$$

$$\sigma_i = \begin{bmatrix} \sigma_i^I & \sigma_i^{IO} \\ \sigma_i^{OI} & \sigma_i^O \end{bmatrix} = \begin{bmatrix} \sigma_i^{xx} & \sigma_i^{x\dot{x}} \\ \sigma_i^{x\dot{x}} & \sigma_i^{\dot{x}\dot{x}} \end{bmatrix} \quad (9)$$

where ξ_t includes the input variable ξ_t^I and the output variable ξ_t^O . μ_i and σ_i are the mean and variance related to the input and output.

E. Probability Calculation

According to the given model $\lambda = \{\pi, A, \{\mu, \sigma\}, \{\mu^C, \sigma^C\}\}$ and observation sequence $V = [v_1, v_2, v_3, \dots, v_M]$, the probability of observation sequence V in the model λ can be calculated by using the forward algorithm as [26]

$$\alpha_{i,t} = P(v_1, v_2, v_3, \dots, v_t, i_t = q_i | \lambda). \quad (10)$$

For $t = 1, 2, 3, \dots, T - 1$, it can be obtained as

$$\alpha_{i,t} = \sum_{j=1}^N \sum_{c=1}^{\min(c^{\max}, t-1)} \alpha_i^j a_{ji} p_i^C(c) \prod_{s=t-c+1}^t \mathcal{N}(\xi_s | \hat{\mu}_i, \hat{\sigma}_i) \quad (11)$$

where $i = 1, 2, 3, \dots, N$. $\alpha_{i,t}$ is the forward probability $P(V | \lambda)$ in state i at time t and $V = (v_1, v_2, v_3, \dots, v_t)$. a_{ji} is the transition probability from the state j at time t to the state i at time t .

F. Reproduction

Based on the probability calculation of HSMM-GMR, a normalized parameter h_i to describe the influence of state i is defined as

$$h_{i,t} = \frac{\alpha_{i,t}}{\sum_{k=1}^N \alpha_{k,t}} \quad (12)$$

$$\alpha_{k,t} = \left(\sum_{k=1}^N \alpha_{k,t-1} a_{ki} \right) \mathcal{N}(\xi_t | \hat{\mu}_i, \hat{\sigma}_i) \quad (13)$$

where $\alpha_{k,t}$ is defined in (11).

From (12) to (13), we have

$$h_{i,t} = \frac{\alpha_{i,t}}{\sum_{k=1}^N \alpha_{k,t}} = \frac{\mathcal{N}(\xi_t | \hat{\mu}_i, \hat{\sigma}_i)}{\sum_{k=1}^N \mathcal{N}(\xi_t | \hat{\mu}_k, \hat{\sigma}_k)}. \quad (14)$$

Inspired by the work in [24], [42], and [43], the current target variable \dot{x} (velocity) can be obtained as

$$\dot{x}^* = \sum_{i=1}^N h_{i,t} \{ [A_i \ b_i] [x_t \ 1]^T \} \quad (15)$$

with

$$A_i = \sigma_i^{xx} (\sigma_i^{xx})^{-1} \quad (16)$$

$$b_i = \hat{\mu}_i^x - \sigma_i^{xx} (\sigma_i^{xx})^{-1} \mu_i^x. \quad (17)$$

According to (15)–(18), we can compute the velocity of the end-manipulator.

It is assumed that the position is known at time t . Motivated by the work in [24], the position can be computed at time $t+1$ by integration

$$\begin{aligned} x^*|_{i=t+1} &= x^*|_{i-1=t} + \mathcal{T} \dot{x}^* \\ &= x^*|_{i-1=t} + \sum_{i=1}^N h_{i,t} \{ [A_i \ b_i] [x_t \ 1]^T \} \end{aligned} \quad (18)$$

where \mathcal{T} is a length of the single iteration time step.

IV. TELEOPERATION CONTROL DESIGN

A. System Dynamics

In this paper, the dynamics of the teleoperation system are described as [44]

$$\begin{cases} M_m(q_m) \ddot{x}_m + C_m(q_m, \dot{q}_m) \dot{x}_m + G_m(q_m) = F_m \\ M_s(q_s) \ddot{q}_s + C_s(q_s, \dot{q}_s) \dot{q}_s + G_s(q_s) = \tau_s \end{cases} \quad (19)$$

where $\{M_m(q_m) \in R^{N_m \times N_m}, C_m(q_m, \dot{q}_m) \in R^{N_m \times N_m}, G_m(q_m) \in R^{N_m}\}$, and $\{M_s(q_s) \in R^{N_s \times N_s},$

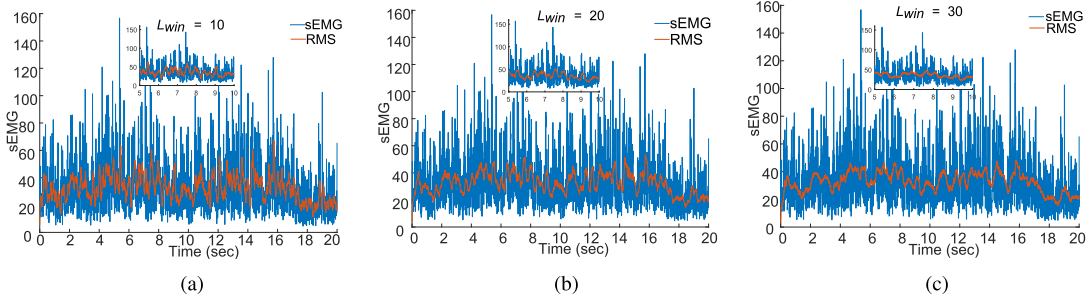


Fig. 6. (a) sEMG signal processing process with $L_{win} = 10$. (b) sEMG signal processing with $L_{win} = 20$. (c) Length of moving window for sEMG signal is $L_{win} = 30$.

$C_s(q_s, \dot{q}_s) \in R^{N_s \times N_s}$, $G_s(q_s) \in R^{N_s}$ are the inertia matrix, Coriolis and centrifugal matrix, and gravitational matrix for the master and the slave in the joint space, respectively. q_m and q_s are the joint angle vector for the master and the slave. $F_m \in R^{N_m}$ is the force of the master in the process of human operation. $\tau_s \in R^{N_s}$ is the control torque of the slave device. N_m and N_s are the DOFs of the master and the slave.

B. Control Strategy

1) *Basic Control*: The potential difference (PD) control methods are both applied in the system for the master and the slave, which are described in

$$\begin{cases} \tau_m = K_{pm}e_m + K_{dm}\dot{e}_m \\ \tau_s = K_{ps}e_s + K_{ds}\dot{e}_s \end{cases} \quad (20)$$

where $e_m = x_{md} - x_m$, $e_s = x_{sd} - x_s$. $\{K_{pm}, K_{dm}\}$ and $\{K_{ps}, K_{ds}\}$ are the proportional term and the differential term of the controller for the master and the slave, respectively.

2) *Task Space Control*: Based on the Denavit–Hartenburg (D–H) parameters of the slave device, the closed-loop inverse kinematics method is introduced to avoid kinematic singularities and numerical drifts for the Cartesian position task. The slave joint velocity q_s can be presented as [44]

$$q_s = \int K_{sp} J_s^T(q_s) e_s \quad (21)$$

with

$$e_s = x_m - x_s = x_{sd} - x_s$$

where K_{sp} and $J_s^T(q_s)$ are the positive definite matrix and the Jacobian matrix for the slave, respectively. e_s is the position error.³

3) *Variable Gain Control*: When the human operator manipulates a telerobot to perform a task, the muscle activation of hand will change according to the feedback from the robot. Thus, a variable gain control method based on the muscle activation is used to enhance the telerobot control performance [37], [44], [45]

$$K^\alpha = (K_{\max}^\alpha - K_{\min}^\alpha) \frac{(\alpha_i^k - \alpha_{\max}^k)}{(\alpha_{\min}^k - \alpha_{\max}^k)} + K_{\min}^\alpha \quad (22)$$

³For simplicity, we just describe the control strategy in the *Learning* phase. The variables x_{sd} , x_s indicate the status of the teleoperated robot in the *Learning* phase.

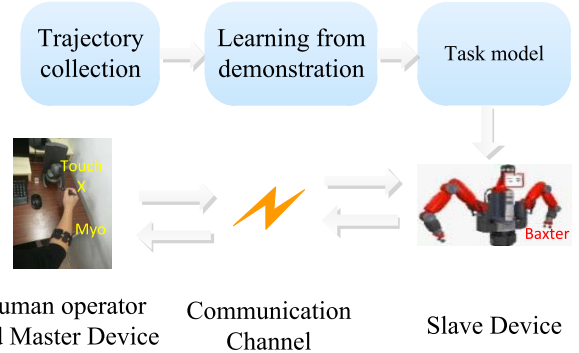


Fig. 7. Experimental setup for a pulling the cotter pin task.

where $a(i) = (e^{A_{emg}u(i)} - 1)(e^{A_{emg}} - 1)$, $u(i)$ are sEMG signal. A_{emg} represents the parameter of muscle activation. K_{\max}^α indicates the maximum of K^α and K_{\min}^α represents the minimum of K^α , i.e., $K_{\min}^\alpha \leq K^\alpha \leq K_{\max}^\alpha$. α_{\min}^k and α_{\max}^k are the upper bound and the lower bound of the muscle activation, respectively.

4) *Tracking Force*: In the process of task execution,⁴ the tracking force F_{tr} varies with the position error of the slave. A PD controller is used to compute the tracking force

$$F_{tr} = K_{ptr}(x_g - x^*) + K_{dtr}\dot{x}^* \quad (23)$$

where K_{ptr} and K_{dtr} are the parameters of the PD controller. x^* and \dot{x}^* are the position and velocity of the end-effector of the slave. x_g is the given desired position.

V. RESULTS

A. sEMG Signal Preprocessing

In this paper, the length of moving window L_{win} is used to evaluate the performance of the rms based on muscle activation.

As shown in Fig. 6(a)–(c), the length of the sampling window has greatly affected the envelope of the sEMG signal.⁵

⁴In the *reproduction* phase, x^* is used as the reference signal for the slave. The parameters of the controller are the same in the *reproduction* phase and *Learning* phase.

⁵It is natural that more samples are used in the moving window the smoother signal will be got. But large computing time and high-frequency information loss as the tradeoff in the process of sEMG signal preprocessing. Therefore, it needs more investigation on the choice of window size in the future.

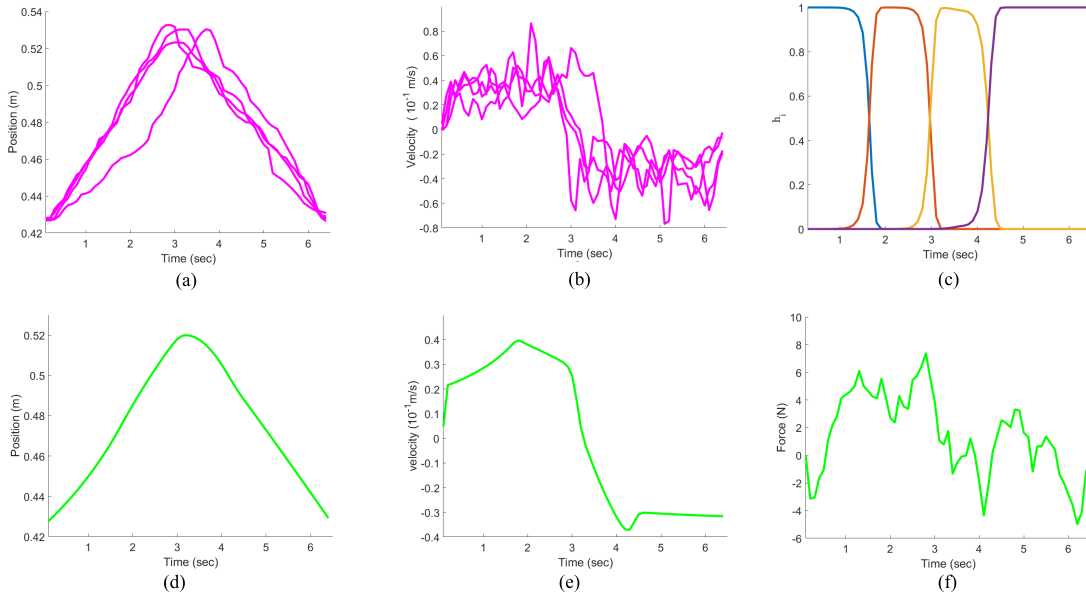


Fig. 8. (a) Recorded position from four demonstrations. (b) Velocity by human operator demonstration. (c) HSMM component activation for the pulling the cotter pin task. (d) Reproduced position in the *reproduction* phase. (e) Velocity in the *reproduction* phase. (f) Tracking force in the *reproduction* phase for the pulling the cotter pin task.

In Fig. 6(a), the envelop curve (red) involves high-frequency characteristic and brings disturbance in the applications. When $L_{win} = 30$, the rms is of a smooth trend as shown in Fig. 6(c); however, the computing time is relatively longer for rms and it cannot meet the requirement for a real-time classifier. Compared with Fig. 6(a) and (c), the curve of the rms is of suitable smoothness and reasonable computing time with $L_{win} = 20$.

B. Semi-Physical Experiment: Pulling the Cotter Pin Task

1) *Semi-Physical Experiment Setting*: In this paper, the proposed method is presented to show the process of robot learning and human intention insertion for the teleoperation system which utilizes a master-slave structure. As shown in Fig. 7, the experimental platform consists of a 6-DOF Touch X haptic device as the master and a virtual Baxter robot as the slave. The experimental facilities communications through a single computer with Windows 7, MATLAB, and Visual Studio 2013. The first part of the experiment is the trajectory tracking to verify the motion performance for a heterogeneous master-slave robotic system. The slave device follows the motion of the master through a communication channel. The second part of the experiment is the pulling the cotter pin task. In the *learning* phase, the task workspace trajectories are recorded as demonstrated observation. Observations are obtained by remotely manipulating the six degrees of freedom slave device. Through manipulation task group, a generative model $\{\pi, A, \{\mu, \sigma\}, \{\mu^C, \sigma^C\}\}$ is obtained by using HSMM-GMM. In the *reproduction* phase, the robot reproduction trajectory can be corrected based on the learned model (HSMM-GMR). In the experiment, the designed controller parameters are presented in Table I. The sampling time for the teleoperated system

TABLE I
DESIGNED CONTROLLER PARAMETERS FOR
THE TELEOPERATED SYSTEM

Parameters	Master device	Slave device
K_{pi}	$K_{pm} = 50$	$K_{ps} = 50$
K_{di}	$K_{dm} = 50$	$K_{ds} = 50$

$t = 0.01$ s, the parameter involves muscle activation is chosen as $A_{emg} = -0.6981$.

2) *Learning Model Through Demonstrations*: This experiment aims at learning a task model to enhance the robot intelligence for the teleoperation system. The trajectory observations of the slave are collected from several demonstration ($C = 4$) by the same human operator using the haptic device. Then, HSMM-GMM method is applied to encode the demonstrations. The number of Gaussian is chosen according to the task segmentation. The hidden states for a pulling the cotter pin task are set $N = 4$.

As shown in Fig. 8(a)–(b), the recorded trajectories of position and velocities of the robot end-effector are demonstrated by the human operator with four demonstrations in the task space. According to (14) and Fig. 8(c), the HSMM component activation curves are computed for pulling the cotter pin task in the *learning* phase.

3) *Reproduction Based on Learned Task Model*: A learned task model can be obtained in *learning* phase. In *reproduction* phase, the learned task model can be adapted according to the task initial conditions. From (15) to (18), the current position/velocity of the robot end-effector can be computed based on the learned task model. Fig. 8(d)–(e) shows the position and the velocity of reproduction for the pulling the cotter pin task. It can be seen that a relative smooth trend in the *reproduction*

TABLE II
RMSEs FOR THE PULLING THE COTTER PIN TASK INVOLVES HUMAN OPERATOR DEMONSTRATIONS

RMSE	Position	Velocity
Pulling the cotter pin task	0.0022	0.0788



Fig. 9. Experimental setup for a drawing task.

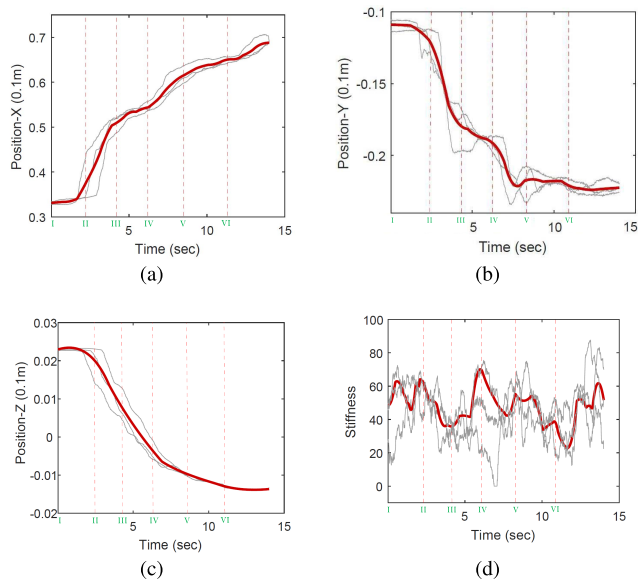


Fig. 10. (a) Position of the robot in x -coordinate during the drawing task. (b) Position of the robot in y -coordinate during the drawing task. (c) Position of the robot in z -coordinate during the drawing task. (d) Stiffness of the human during the drawing task.

phase in comparison with the human operator demonstrations. As shown in Fig. 8(f), the tracking force is computed in (23).

The root-mean-square errors (RMSEs) show the accuracy of the proposed method in *reproduction* phase in Table II. The RMSEs value indicates that the superiority of the proposed reproduction method based on the learned task model.

C. Experiment: Drawing Task

The purpose of this experiment is to evaluate the performance of the presented method in a simple task.

1) *Experiment Setting*: In this experiment, a typical drawing task is performed by the teleoperation system as presented in Fig. 9. In this experiment, a green pen is attached onto the

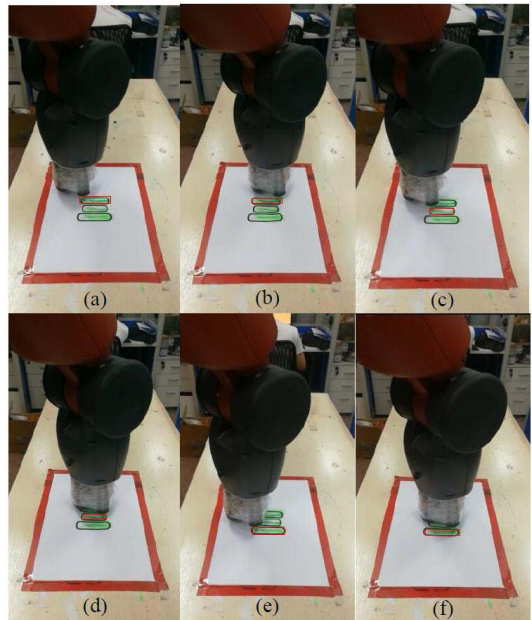


Fig. 11. Robot execution for a drawing task.

endpoint of the slave right arm as a drawing tool. A human operator manipulates the master device to teleoperate the end-effector of the slave to perform a drawing task. We collect $C = 3$ demonstrations and train $N = 18$ states of the HSMM in the *learning* phase. We then perform a drawing task in a 210 mm \times 297 mm (A4) 2-D space.

2) *Results and Analysis*: The motion trajectories and stiffness profile of the drawing task are shown in Fig. 10(a)–(c). The gray curves indicate the demonstration results. The red curve represents the result of preproduction. The *reproduction* phase can be divided into six steps (I–VI). In steps I and II, the robot begins to perform a subtask drawing task 1. In steps II and III, the end-effector of the slave leaves from the paper for another drawing operation. Similarly, subtask drawing task 2 and subtask drawing task 3 are performed in steps III and IV and steps V and VI, respectively. During the *learning* phase, humans’ stiffness is variable which follows with the drawing operation. As shown in Fig. 10(d), humans’ stiffness maintains a high level in steps I and II, III and IV, and V and VI.

In Fig. 11, the telerobot performs the drawing task by using a reproduced stiffness. From Fig. 11(a)–(f), it can be concluded that the drawing tasks are successfully performed by employing the proposed method.

VI. CONCLUSION

The purpose of this paper is to explore a mapping of relationship to represent the task model between the perception information and the robot learning method. This paper proposed a novel algorithm integrating the haptics EMG perception mechanism and robot learning based on HSMM and GMM/GMR. The human operator could adjust the muscle activation according to the HRI environment and this muscle activation process could be observed and recorded.

By utilizing the recorded sEMG signal and a task learning framework, the teleoperation system could naturally interact with the external environment and encode the demonstrations and reproduction of the HRI task to enhance the robot intelligence, respectively. Experimental results have demonstrated the effectiveness of the proposed haptic feedback with sEMG-based variable gain control mechanism and the robot learning method. In the future work, we will introduce the force information of the robot's end-effector and vision information into the telerobot perception system to construct the multimodal information fusion platform. Moreover, we will exploit the more effective task learning model for the enhancement of the robot intelligence in the teleoperated areas.

REFERENCES

- [1] C. Yang, K. Huang, H. Cheng, Y. Li, and C.-Y. Su, "Haptic identification by ELM-controlled uncertain manipulator," *IEEE Trans. Syst., Man, Cybern., Syst.*, vol. 47, no. 8, pp. 2398–2409, Aug. 2017.
- [2] C. Yang, C. Zeng, P. Liang, Z. Li, R. Li, and C.-Y. Su, "Interface design of a physical human–robot interaction system for human impedance adaptive skill transfer," *IEEE Trans. Autom. Sci. Eng.*, vol. 15, no. 1, pp. 329–340, Jan. 2018.
- [3] J. Huang, Y. Wang, and T. Fukuda, "Set-membership-based fault detection and isolation for robotic assembly of electrical connectors," *IEEE Trans. Autom. Sci. Eng.*, vol. 15, no. 1, pp. 160–171, Jan. 2018.
- [4] J. Huang, W. Huo, W. Xu, S. Mohammed, and Y. Amirat, "Control of upper-limb power-assist exoskeleton using a human-robot interface based on motion intention recognition," *IEEE Trans. Autom. Sci. Eng.*, vol. 12, no. 4, pp. 1257–1270, Oct. 2015.
- [5] H. Liu, Y. Wu, F. Sun, B. Fang, and D. Guo, "Weakly paired multimodal fusion for object recognition," *IEEE Trans. Autom. Sci. Eng.*, vol. 15, no. 2, pp. 784–795, Apr. 2018.
- [6] J. Su, H. Qiao, Z. Ou, and Z. Y. Liu, "Vision-based caging grasps of polyhedron-like workpieces with a binary industrial gripper," *IEEE Trans. Autom. Sci. Eng.*, vol. 12, no. 3, pp. 1033–1046, Jul. 2015.
- [7] L. Peternel, T. Petrič, and J. Babič, "Human-in-the-loop approach for teaching robot assembly tasks using impedance control interface," in *Proc. IEEE Int. Conf. Robot. Autom.*, May 2015, pp. 1497–1502.
- [8] H. Liu, F. Sun, B. Fang, and X. Zhang, "Robotic room-level localization using multiple sets of sonar measurements," *IEEE Trans. Instrum. Meas.*, vol. 66, no. 1, pp. 2–13, Jan. 2017.
- [9] J. Su, H. Qiao, C. Liu, Y. Song, and A. Yang, "Grasping objects: The relationship between the cage and the form-closure grasp," *IEEE Robot. Autom. Mag.*, vol. 24, no. 3, pp. 84–96, Sep. 2017.
- [10] Z. Liu, J. Luo, L. Wang, Y. Zhang, C. L. P. Chen, and X. Chen, "A time-sequence-based fuzzy support vector machine adaptive filter for tremor cancelling for microsurgery," *Int. J. Syst. Sci.*, vol. 46, no. 6, pp. 1131–1146, 2015.
- [11] Z. Liu, C. Mao, J. Luo, Y. Zhang, and C. L. P. Chen, "A three-domain fuzzy wavelet network filter using fuzzy PSO for robotic assisted minimally invasive surgery," *Knowl.-Based Syst.*, vol. 66, pp. 13–27, Aug. 2014.
- [12] H. Liu, F. Sun, B. Fang, and S. Lu, "Multimodal measurements fusion for surface material categorization," *IEEE Trans. Instrum. Meas.*, vol. 67, no. 2, pp. 246–256, Feb. 2018.
- [13] R. Li and H. Qiao, "Condition and strategy analysis for assembly based on attractive region in environment," *IEEE/ASME Trans. Mechatronics*, vol. 22, no. 5, pp. 2218–2228, Oct. 2017.
- [14] H. Liu, J. Qin, F. Sun, and D. Guo, "Extreme kernel sparse learning for tactile object recognition," *IEEE Trans. Cybern.*, vol. 47, no. 12, pp. 4509–4520, Dec. 2017.
- [15] R. Chalodhorn, D. B. Grimes, K. Grochow, and R. P. N. Rao, "Learning to walk through imitation," in *Proc. IJCAI*, vol. 7, 2007, pp. 2084–2090.
- [16] N. Koenig and M. J. Matarić, "Robot life-long task learning from human demonstrations: A Bayesian approach," *Auto. Robots*, vol. 41, no. 5, pp. 1173–1188, 2017.
- [17] D. H. Grollman and O. C. Jenkins, "Dogged learning for robots," in *Proc. IEEE Int. Conf. Robot. Autom.*, Apr. 2007, pp. 2483–2488.
- [18] T. Inamura, N. Kojo, T. Sonoda, K. Sakamoto, K. Okada, and M. Inaba, "Intent imitation using wearable motion capturing system with on-line teaching of task attention," in *Proc. 5th IEEE-RAS Int. Conf. Humanoid Robots*, Dec. 2005, pp. 469–474.
- [19] A. Hussein, M. M. Gaber, E. Elyan, and C. Jayne, "Imitation learning: A survey of learning methods," *ACM Comput. Surv.*, vol. 50, no. 2, 2017, Art. no. 21.
- [20] M. Field, D. Stirling, Z. Pan, and F. Naghdy, "Learning trajectories for robot programming by demonstration using a coordinated mixture of factor analyzers," *IEEE Trans. Cybern.*, vol. 46, no. 3, pp. 706–717, Mar. 2016.
- [21] A. Vakanski, I. Mantegh, A. Irish, and F. Janabi-Sharifi, "Trajectory learning for robot programming by demonstration using hidden Markov model and dynamic time warping," *IEEE Trans. Syst., Man, Cybern. B, Cybern.*, vol. 42, no. 4, pp. 1039–1052, Aug. 2012.
- [22] X. Yin and Q. Chen, "Trajectory generation with spatio-temporal templates learned from demonstrations," *IEEE Trans. Ind. Electron.*, vol. 64, no. 4, pp. 3442–3451, Apr. 2017.
- [23] M. Deniša, A. Gams, A. Ude, and T. Petrič, "Learning compliant movement primitives through demonstration and statistical generalization," *IEEE/ASME Trans. Mechatronics*, vol. 21, no. 5, pp. 2581–2594, Oct. 2016.
- [24] M. Racca, J. Pajarinen, A. Montebelli, and V. Kyrki, "Learning in-contact control strategies from demonstration," in *Proc. IEEE/RSJ Int. Conf. Intell. Robots Syst. (IROS)*, Oct. 2016, pp. 688–695.
- [25] L. Rozo, P. Jiménez, and C. Torras, "Force-based robot learning of pouring skills using parametric hidden Markov models," in *Proc. IEEE 9th Workshop Robot Motion Control (RoMoCo)*, Jul. 2013, pp. 227–232.
- [26] A. K. Tanwani and S. Calinon, "Learning robot manipulation tasks with task-parameterized semitied hidden semi-Markov model," *IEEE Robot. Autom. Lett.*, vol. 1, no. 1, pp. 235–242, Jan. 2016.
- [27] A. K. Tanwani and S. Calinon. (2016). "Small variance asymptotics for non-parametric online robot learning." [Online]. Available: <https://arxiv.org/abs/1610.02468>
- [28] K. Khokar, R. Alqasemi, S. Sarkar, K. Reed, and R. Dubey, "A novel telerobotic method for human-in-the-loop assisted grasping based on intention recognition," in *Proc. IEEE Int. Conf. Robot. Autom. (ICRA)*, May/June 2014, pp. 4762–4769.
- [29] N. Stefanov, A. Peer, and M. Buss, "Online intention recognition for computer-assisted teleoperation," in *Proc. IEEE Int. Conf. Robot. Autom. (ICRA)*, May 2010, pp. 5334–5339.
- [30] Z. Wang *et al.*, "Probabilistic movement modeling for intention inference in human-robot interaction," *Int. J. Robot. Res.*, vol. 32, no. 7, pp. 841–858, 2013.
- [31] G. Maeda, G. Neumann, M. Ewerton, R. Lioutikov, and J. Peters, "A probabilistic framework for semi-autonomous robots based on interaction primitives with phase estimation," in *Robotics Research*, Cham, Switzerland: Springer, 2018, pp. 253–268.
- [32] H. C. Ravichandar and A. P. Dani, "Human intention inference using expectation-maximization algorithm with online model learning," *IEEE Trans. Autom. Sci. Eng.*, vol. 14, no. 2, pp. 855–868, Apr. 2017.
- [33] L. Peternel, E. Oztop, and J. Babič, "A shared control method for online human-in-the-loop robot learning based on locally weighted regression," in *Proc. IEEE/RSJ Int. Conf. Intell. Robots Syst. (IROS)*, Oct. 2016, pp. 3900–3906.
- [34] C. J. Pérez-del-Pulgar, J. Smisek, V. F. Muñoz, and A. Schiele, "Using learning from demonstration to generate real-time guidance for haptic shared control," in *Proc. IEEE Int. Conf. Syst., Man, Cybern.*, Oct. 2016, pp. 003205–003210.
- [35] A. Pervez, A. Ali, J.-H. Ryu, and D. Lee, "Novel learning from demonstration approach for repetitive teleoperation tasks," in *Proc. IEEE World Haptics Conf.*, Jun. 2017, pp. 60–65.
- [36] J. Su, "Representation and inference of user intention for Internet robot," *IEEE Trans. Syst., Man, Cybern., Syst.*, vol. 44, no. 8, pp. 995–1002, Aug. 2014.
- [37] C. Yang, J. Luo, Y. Pan, Z. Liu, and C.-Y. Su, "Personalized variable gain control with tremor attenuation for robot teleoperation," *IEEE Trans. Syst., Man, Cybern. A, Syst.*, vol. 48, no. 10, pp. 1759–1770, Oct. 2018.
- [38] G. R. Naik, S. E. Selvan, M. Gobbo, A. Acharyya, and H. T. Nguyen, "Principal component analysis applied to surface electromyography: A comprehensive review," *IEEE Access*, vol. 4, pp. 4025–4037, 2016.
- [39] G. Biagetti, P. Crippa, S. Orcioni, and C. Turchetti, "Homomorphic deconvolution for MUAP estimation from surface EMG signals," *IEEE J. Biomed. Health Informat.*, vol. 21, no. 2, pp. 328–338, Mar. 2017.
- [40] L. Rozo, J. Silvério, S. Calinon, and D. G. Caldwell, "Learning controllers for reactive and proactive behaviors in human–robot collaboration," *Frontiers Robot. AI*, vol. 3, no. 30, pp. 1–11, 2016.
- [41] A. K. Tanwani and S. Calinon, "A generative model for intention recognition and manipulation assistance in teleoperation," in *Proc. IEEE/RSJ Int. Conf. Intell. Robots Syst. (IROS)*, Sep. 2017, pp. 43–50.

- [42] S. Calinon, A. Pistillo, and D. G. Caldwell, "Encoding the time and space constraints of a task in explicit-duration hidden Markov model," in *Proc. IEEE/RSJ Int. Conf. Intell. Robots Syst. (IROS)*, Sep. 2011, pp. 3413–3418.
- [43] S. Calinon and A. Billard, "Statistical learning by imitation of competing constraints in joint space and task space," *Adv. Robot.*, vol. 23, no. 15, pp. 2059–2076, 2009.
- [44] C. Yang, X. Wang, Z. Li, Y. Li, and C.-Y. Su, "Teleoperation control based on combination of wave variable and neural networks," *IEEE Trans. Syst., Man, Cybern., Syst.*, vol. 47, no. 8, pp. 2125–2136, Aug. 2017.
- [45] C. Yang, Y. Jiang, Z. Li, W. He, and C.-Y. Su, "Neural control of bimanual robots with guaranteed global stability and motion precision," *IEEE Trans. Ind. Informat.*, vol. 13, no. 3, pp. 1162–1171, Jun. 2017.



Chenguang Yang (M'10–SM'16) received the B.Eng. degree in measurement and control from Northwestern Polytechnical University, Xi'an, China, in 2005, and the Ph.D. degree in control engineering from the National University of Singapore, Singapore, in 2010.

He was a Post-Doctoral Fellow with the Imperial College London, London, U.K. His research interests include robotics and automation.

Dr. Yang was a recipient of the Best Paper Award in the IEEE TRANSACTIONS ON ROBOTICS and a

number of international

Jing Luo (S'17) is currently pursuing the Ph.D. degree with the South China University of Technology, Guangzhou, China.

His research interests include robotics, teleoperation, haptics, nonlinear control theory, machine learning, and human–robot interaction.



Chao Liu (S'02–M'05–SM'13) received the Ph.D. degree in electrical and electronic engineering from Nanyang Technological University, Singapore, in 2006.

He is currently a CR Research Scientist with the French National Center for Scientific Research (CNRS), Department of Robotics, LIRMM, University of Montpellier-CNRS, Montpellier, France. His research interests include surgical robotics, teleoperation, haptics, nonlinear control theory, and applications.



Miao Li received the bachelor's and master's degrees from the School of Mechanical Science and Engineering, Huazhong University of Science and Technology, Wuhan, China, in 2008 and 2011, respectively.

In 2011, he joined the Department of Mechanical Engineering, Ecole Polytechnique Federale de Lausanne, Lausanne, Switzerland, as a Doctoral Assistant. His research interests include robust robotic grasping and impedance control of dexterous manipulation using tactile sensing.



Shi-Lu Dai (S'09–M'11) received the B.Eng. degree in thermal engineering and the M.Eng. and Ph.D. degrees in control science and engineering from Northeastern University, Shenyang, China, in 2002, 2006, and 2010, respectively.

From 2007 to 2009, he was a Visiting Student with the Department of Electrical and Computer Engineering, National University of Singapore, Singapore. From 2015 to 2016, he was a Visiting Scholar with the Department of Electrical Engineering, University of Notre Dame, Notre Dame, IN, USA.

Since 2010, he has been with the School of Automation Science and Engineering, South China University of Technology, Guangzhou, China, where he is currently a Professor. His research interests include adaptive and learning control and distributed cooperative systems.